

# Oxygen Activation by Co(II) and a Redox Non-Innocent Ligand: Spectroscopic Characterization of a Radical–Co(II)–Superoxide Complex with Divergent Catalytic Reactivity

Amanda R. Corcos,<sup>†</sup> Omar Villanueva,<sup>‡,∇</sup> Richard C. Walroth,<sup>§</sup> Savita K. Sharma,<sup>‡</sup> John Bacsa,<sup>‡</sup> Kyle M. Lancaster,<sup>\*,§</sup> Cora E. MacBeth,<sup>\*,‡</sup> and John F. Berry<sup>\*,†</sup>

<sup>†</sup>Department of Chemistry, University of Wisconsin-Madison, 1101 University Ave., Madison, Wisconsin 53706, United States

<sup>‡</sup>Department of Chemistry, Emory University, 1515 Dickey Drive, Atlanta, Georgia 30322, United States

<sup>§</sup>Department of Chemistry and Chemical Biology, Baker Laboratory, Cornell University, Ithaca, New York 14853, United States

## Supporting Information

**ABSTRACT:** Bimetallic  $(\text{Et}_4\text{N})_2[\text{Co}_2(\text{L})_2]$ ,  $(\text{Et}_4\text{N})_2[\mathbf{1}]$  (where  $(\text{L})^{3-} = (\text{N}(o\text{-PhNC}(\text{O})^i\text{Pr})_2)^{3-}$ ) reacts with 2 equiv of  $\text{O}_2$  to form the monometallic species  $(\text{Et}_4\text{N})[\text{Co}(\text{L})\text{O}_2]$ ,  $(\text{Et}_4\text{N})[\mathbf{3}]$ . A crystallographically characterized analog  $(\text{Et}_4\text{N})_2[\text{Co}(\text{L})\text{CN}]$ ,  $(\text{Et}_4\text{N})_2[\mathbf{2}]$ , gives insight into the structure of  $[\mathbf{3}]^{1-}$ . Magnetic measurements indicate  $[\mathbf{2}]^{2-}$  to be an unusual high-spin  $\text{Co}^{\text{II}}$ -cyano species ( $S = 3/2$ ), while IR, EXAFS, and EPR spectroscopies indicate  $[\mathbf{3}]^{1-}$  to be an end-on superoxide complex with an  $S = 1/2$  ground state. By X-ray spectroscopy and calculations,  $[\mathbf{3}]^{1-}$  features a high-spin  $\text{Co}^{\text{II}}$  center; the net  $S = 1/2$  spin state arises after the Co electrons couple to both the  $\text{O}_2^{\bullet-}$  and the aminyl radical on redox non-innocent  $(\text{L}^{\bullet})^{2-}$ . Dianion  $[\mathbf{1}]^{2-}$  shows both nucleophilic and electrophilic catalytic reactivity upon activation of  $\text{O}_2$  due to the presence of both a high-energy, filled  $\text{O}_2^- \pi^*$  orbital and an empty low-lying  $\text{O}_2^- \pi^*$  orbital in  $[\mathbf{3}]^{1-}$ .

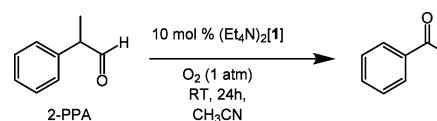
Synthetic cobalt complexes have been known to bind  $\text{O}_2$  since the days of Werner.<sup>1</sup> Upon  $\text{O}_2$  addition, most  $\text{Co}^{\text{II}}$  complexes form kinetically inert low-spin  $\text{Co}^{\text{III}}$  terminal superoxide or  $\mu$ -peroxide compounds that are inactive in catalysis.<sup>2</sup> Catalytic reactivity can be coaxed from such molecules by addition of a coreductant.<sup>2i,3</sup> In contrast, nature uses multiple metal centers<sup>4</sup> or redox non-innocent ligands<sup>5</sup> to supply the requisite electrons when activating  $\text{O}_2$  for catalysis with first-row transition-metal complexes.

We recently reported<sup>6</sup> the dimeric pseudotetrahedral  $\text{Co}^{\text{II}}$  complex  $(\text{Et}_4\text{N})_2[\text{Co}_2(\text{L})_2]$ ,  $(\text{Et}_4\text{N})_2[\mathbf{1}]$  (where  $\text{L} = (\text{N}(o\text{-PhNC}(\text{O})^i\text{Pr})_2)^{3-}$ ), which is unique among  $\text{Co}^{\text{II}}$  compounds for its ability to activate  $\text{O}_2$  toward electrophilic O-atom transfer without supplemental coreductants. This  $\text{O}_2$  activation proceeds with dioxygenase stoichiometry.<sup>6</sup> Here, we explore additional reactivity and offer insights into the  $\text{O}_2$  activation step for this catalyst by characterizing the intermediate formed upon its interaction with  $\text{O}_2$ . Our discussion is facilitated by comparison to a stable compound formed using  $\text{CN}^-$  as an  $\text{O}_2$  analog. Surprisingly, instead of forming a kinetically inert, low-spin  $\text{Co}^{\text{III}}$  species, we show that the  $\text{Co}^{\text{II}}$  centers remain high-spin when either substrate is added. Consequently, we argue

that  $\text{O}_2$  reduction occurs via one-electron oxidation of L rather than Co.

In addition to its behavior as a catalyst for aerobic O-atom transfer,<sup>6</sup> we have now found  $(\text{Et}_4\text{N})_2[\mathbf{1}]$  to be an excellent catalyst for the aerobic deformylation of 2-phenylpropionaldehyde (2-PPA), forming acetophenone in good yields (Scheme 1). While biological systems are known to carry out catalytic

**Scheme 1. Catalytic Aerobic Deformylation of 2-PPA by  $(\text{Et}_4\text{N})_2[\mathbf{1}]$**



deformylation (nucleophilic) reactions using  $\text{O}_2$ ,<sup>7</sup> synthetic aerobic deformylation catalysts have, to the best of our knowledge, not yet been reported.<sup>8,9</sup> Metal-oxygen species typically show either electrophilic or nucleophilic character; this system merits study due to its electronically divergent reactivity.<sup>10</sup>

To better understand this divergently reactive species, 2 equiv of  $\text{CN}^-$ , an  $\text{O}_2$  surrogate, was added to  $[\mathbf{1}]^{2-}$ .  $\text{CN}^-$  was found to disrupt the bimetallic core structure, yielding 2 equiv of monometallic  $(\text{Et}_4\text{N})_2[\text{Co}(\text{L})\text{CN}]$ ,  $(\text{Et}_4\text{N})_2[\mathbf{2}]$  (Figures 1 and S1–S3), which has been crystallographically characterized as containing a four-coordinate  $\text{Co}^{\text{II}}$  center, at the border between pseudosawhorse and pseudotetrahedral geometry ( $\tau_8 = 0.59$ ).<sup>11</sup> The L ligand backbone undergoes a structural rearrangement upon reaction of  $(\text{Et}_4\text{N})_2[\mathbf{1}]$  with  $\text{CN}^-$  such that each  $(\text{L})^{3-}$  ligand coordinates to a single Co center in a novel tridentate pincer-like coordination mode.<sup>6</sup>

Several spectroscopic techniques were employed to determine the first observable catalytically relevant intermediate responsible for the divergent reactivity of  $[\mathbf{1}]^{2-}$ . Gas-uptake experiments indicate that  $[\mathbf{1}]^{2-}$  reacts with  $\text{O}_2$  in a 1:2 stoichiometry (see SI), suggesting that one molecule of  $\text{O}_2$  is taken up per Co center. UV–vis spectroscopy shows isosbestic behavior, indicating clean conversion of  $[\mathbf{1}]^{2-}$  to  $[\mathbf{3}]^{1-}$  via a

Received: December 3, 2015

Published: January 22, 2016

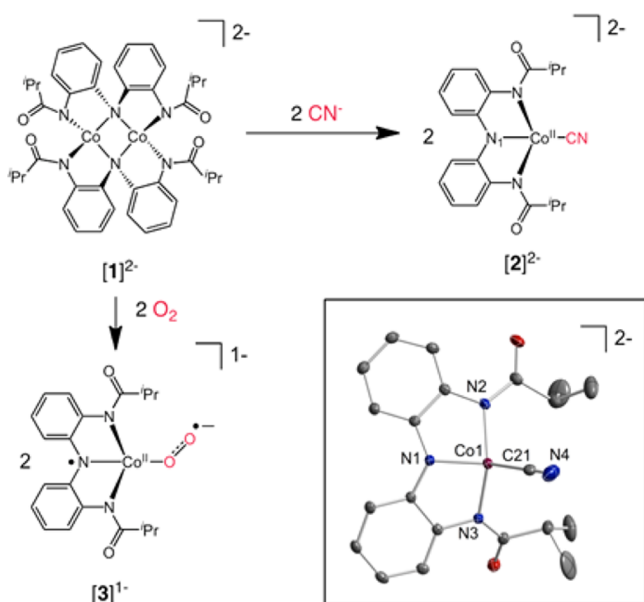


**Figure 1.** Preparation of  $[2]^{2-}$  and  $[3]^{1-}$  from  $[1]^{2-}$ . Thermal ellipsoid plot of  $[2]^{2-}$  is shown at the 45% probability level, with H atoms and counter cations omitted for clarity.

short-lived intermediate (Figure S4). The resulting burgundy species  $[3]^{1-}$  can be isolated or used in situ to perform stoichiometric oxidations with  $\text{PPh}_3$  and 2-PPA, generating the same products of catalytic oxidations using  $[1]^{2-}$  (see SI). Along with the monometallic structure of  $(\text{Et}_4\text{N})_2[2]$ , this result suggests that  $[1]^{2-}$  reacts with  $\text{O}_2$  to form a monometallic  $\text{Co}-\text{O}_2$  species,  $[\text{Co}(\text{L})\text{O}_2]^{1-}$ ,  $[3]^{1-}$ . The monomeric nature of  $[3]^{1-}$  is further supported by MALDI-TOF mass spectrometry, which shows that new ions with  $m/z = 410.49$  or  $412.47$  amu are produced when  $[1]^{2-}$  reacts with 2 equiv of  $^{16}\text{O}_2$  or  $^{18}\text{O}_2$ , respectively (Figure S5). These mass values are consistent with formulations as  $[3 - ^{16/18}\text{O}]^{1-}$  species, similar to mass spectral data observed for a recently reported five-coordinate  $\text{Co}-\text{O}_2$  complex capable of C–H bond activation via a postulated  $\text{Co}^{\text{IV}}-\text{oxo}$  intermediate.<sup>12</sup> Liquid-cell IR techniques show that  $[3]^{1-}$  has an  $\text{O}_2$  stretching feature at  $1248 \text{ cm}^{-1}$ , which shifts to  $1203 \text{ cm}^{-1}$  upon  $^{18}\text{O}_2$  labeling (Figure S6). These data are consistent with end-on  $\text{Co}-\text{superoxide}$  coordination.<sup>13</sup>

This molecular geometry is further supported by analysis of extended X-ray absorption fine structure (EXAFS) in the Co K-edge XAS of  $[2]^{2-}$  and  $[3]^{1-}$  (Figures S7–8 and Table S1). The EXAFS of  $[2]^{2-}$  and  $[3]^{1-}$  are qualitatively similar, yielding a Co coordination number of four with average Co–L distances of 1.98 and 1.88 Å, respectively. These distances are in good agreement with the crystallographic and DFT-optimized average Co–L distances of 2.01 and 2.04 Å for  $[2]^{2-}$ , respectively, and are also in good agreement with the calculated average Co–L distance for  $[3]^{1-}$  at 1.87 Å. These results suggest a similar coordination geometry for  $(\text{L})^{3-}$  in  $[2]^{2-}$  and  $[3]^{1-}$ , further indicating a monometallic  $\text{Co}(\text{L})$  end-on superoxide structural unit for  $[3]^{1-}$ .

Ground-state electronic configurations of  $[2]^{2-}$  and  $[3]^{1-}$  were established from their magnetic properties. For  $[2]^{2-}$ , the  $\mu_{\text{eff}}$  value of  $4.27(3) \mu_{\text{B}}$  at 298 K in  $\text{CDCl}_3$  is indicative of an  $S = 3/2$  ground state. EPR data (Figure 2a) confirm this unusual high-spin state, with observed (effective)  $g$  values of  $g_x = 4.53$ ,  $g_y = 3.97$ , and  $g_z = 1.95$ , indicating  $D > h\nu$ . Despite the clear

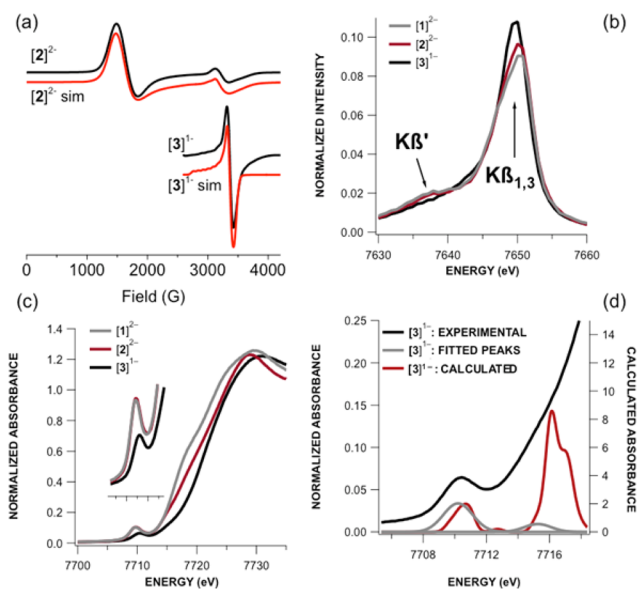


**Figure 2.** (a) Experimental EPR data and simulations for  $[2]^{2-}$  and  $[3]^{1-}$ . (b) Co  $K\beta$  XES main lines of  $[1]^{2-}$ – $[3]^{1-}$ . (c) Co K-edge XANES of  $[1]^{2-}$ – $[3]^{1-}$ . Inset: Magnification of the Co 1s  $\rightarrow$  (Co 3d + L) pre-edge features. (d) Overlay of calibrated TDDFT-calculated (B3LYP/def2-TZVP-ZORA) Co K-edge XANES pre-edge peaks for  $[3]^{1-}$ .

indication of an  $S = 3/2$  ground state for  $[2]^{2-}$ , the EPR spectrum for  $[3]^{1-}$  is surprisingly characteristic of an  $S = 1/2$  species, best simulated by  $g_x = 2.20$ ,  $g_y = 2.00$ ,  $g_z = 1.975$  ( $\mu_{\text{eff}} = 2.13 \mu_{\text{B}}$  at 298 K in  $\text{CH}_3\text{CN}$ ). The observation of a “high-spin” complex of cyanide, a strong-field ligand, is unusual<sup>14</sup> but consistent with the low coordination number. Even more unusual is that the weaker field  $\text{O}_2^-$  complex,  $[3]^{1-}$ , appears low spin. Co  $K\beta$  X-ray emission spectra (XES) of  $[2]^{2-}$  and  $[3]^{1-}$  were measured as a probe of the local spin at Co (Figure 2b). Splitting of  $K\beta$  ( $3p \rightarrow 1s$ ) main lines into  $K\beta'$  and  $K\beta_{1,3}$  features is a useful metric of spin population since electron delocalization out of metal 3d orbitals results in attenuation of the 3d–3p exchange energy.<sup>15</sup>  $K\beta$  main line splitting is markedly decreased in  $[3]^{1-}$  compared to  $[1]^{2-}$  and  $[2]^{2-}$ , consistent with a decreased local Co spin population in  $[3]^{1-}$ .

To defuse this spin-state conundrum, DFT calculations were employed to produce an electronic structure picture consistent with the aggregate structural and spectral data. To this end, we evaluated multiple electronic configurations for  $[2]^{2-}$  and  $[3]^{1-}$ .<sup>16</sup> The quartet state for  $[2]^{2-}$  was energetically favored over the doublet state by 26.7 kJ/mol, in agreement with the EPR data and the similarity of the Co X-ray absorption near-edge spectroscopy (XANES) pre-edge energy of  $[2]^{2-}$  with that of  $[1]^{2-}$ , for the  $\text{Co}^{\text{II}}$  centers in  $[1]^{2-}$  are high-spin<sup>6</sup> (Figure 2c). The optimized geometry for  $[2]^{2-}$  as a quartet is also a superior match to the crystallographic data (Table S5). Additionally, the cyanide  $\text{C}\equiv\text{N}$  stretch predicted to occur at  $2211 \text{ cm}^{-1}$  is experimentally measured at  $2109 \text{ cm}^{-1}$ , in decent agreement given the well-known tendency for DFT to overestimate vibrational frequencies.<sup>17</sup>

For  $[3]^{1-}$ , DFT calculations support an  $S = 1/2$  end-on superoxide species as the configuration with lowest energy (Table S6),<sup>18</sup> in accord with experimental data. For this species, a spin-coupled electronic structure is obtained. There are two low-lying doubly occupied Co-centered  $e$ -type orbitals of the pseudotetrahedral Co d orbital manifold and three singly

occupied orbitals for the  $t_2$ -derived set (Figures 3 and S13). The superoxide ligand has two  $\pi^*$  valence orbitals—doubly

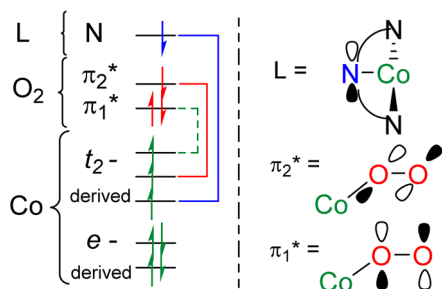


**Figure 3.** Molecular orbital interactions for  $[3]^{1-}$ . (Left) Green, red, and blue arrows represent electrons in Co-, O<sub>2</sub>-, and ligand-based orbitals, respectively. The red and blue brackets show antiferromagnetic coupling between the O<sub>2</sub>- and N-based ligands with Co d electrons. The green dashed bracket shows the three-electron  $\sigma$  interaction between a Co electron and the  $\pi_1^*$  of the O<sub>2</sub><sup>-</sup> ligand. (Right) Representation of ligand- and O<sub>2</sub>-based orbitals.

occupied  $\pi_1^*$  and singly occupied  $\pi_2^*$ —that interact with the Co  $t_2$ -derived orbitals. The  $\pi_1^*$  orbital engages in a three-electron  $\sigma$  interaction with one Co orbital, while the  $\pi_2^*$  unpaired electron is coupled with another Co electron. A second antiferromagnetic interaction exists between the third Co  $t_2$ -derived electron and a ligand-based orbital having significant character from the central N atom of L. Therefore, as with  $[2]^{2-}$ , the metal center in  $[3]^{1-}$  contains a high-spin  $S = 3/2$  Co<sup>II</sup> center. In this case, however, two of the three unpaired electrons of the Co<sup>II</sup> center couple with an L radical and a superoxide radical to yield an overall  $S = 1/2$  ground state. This electronic structure explains the divergent reactivity of (Et<sub>4</sub>N)[3] (vide supra), for the half-filled O<sub>2</sub>  $\pi_2^*$  orbital can be either a donor orbital for nucleophilic reactivity or an acceptor orbital for electrophilic reactivity.

The Co K-edge XANES of  $[1]^{2-}$ – $[3]^{1-}$  (Figure 2c) deserve further comment. All of the other experimental and computational data clearly indicate that the Co<sup>II</sup> oxidation state remains constant throughout this series, but the pre-edge features in the spectra of (Et<sub>4</sub>N)<sub>2</sub>[1] and (Et<sub>4</sub>N)<sub>2</sub>[2] effectively superimpose at 7709.7 eV, while that for  $[3]^{1-}$  is shifted in energy to 7710.2 eV. Furthermore, rising edges distinguish all three compounds from one another, at 7716 eV, 7717.4 eV, and 7720.4 eV for  $[1]^{2-}$ ,  $[2]^{2-}$ , and  $[3]^{1-}$ , respectively (Figure S9).

TD-DFT analysis of XANES pre-edge features, accomplished via calibration to a set of model compounds (Figure S10), was performed to reconcile the XANES features with the electronic structures of  $[1]^{2-}$ – $[3]^{1-}$ . For  $[2]^{2-}$ , this led to a straightforward assignment of the pre-edge transition as arising from the Co 1s to the valence “ $t_2$ ”-derived set. In the case of  $[3]^{1-}$  (Figure 2d), the acceptor orbitals participating in this excitation have substantial O–O  $\pi^*$  admixture. Comparison of the spin density plots of  $[2]^{2-}$  vs  $[3]^{1-}$  shows this effect quite clearly; while the spin density in  $[2]^{2-}$  is highly localized on the metal center with orbitals having roughly 70% metal character, the spin for  $[3]^{1-}$  is more delocalized, and the orbitals are closer to 50% metal in character (Figure S11).

This delocalization of electron density manifests in the calculated Co atomic charges 0.47, 0.55, and 0.64 for  $[1]^{2-}$ ,  $[2]^{2-}$ , and  $[3]^{1-}$ , respectively. These values correlate to a reasonable degree ( $R^2 = 0.94$ ) with the corresponding rising edge inflection points (Figure S9). Moreover, the trend line

extrapolates to  $7706 \pm 3$  eV at a charge of 0, consistent with the rising edge inflection of Co metal (7709 eV). Consequently, variations in the XANES of  $[3]^{1-}$  from the other compounds do not necessarily reflect a change in the physical oxidation state at Co after reaction with O<sub>2</sub>. The difference in energy of the Co K-edge XANES pre-edge features is due to a difference in the nature of the acceptor orbital when comparing  $[1]^{2-}$  and  $[2]^{2-}$  to  $[3]^{1-}$ , as has been seen previously for Cu complexes.<sup>19</sup> The shift to higher energy of the rising edge inflection point in  $[3]^{1-}$  likely reflects the highly covalent interaction of Co with an electronegative O-donor. Although XANES is widely used as a metric of physical oxidation states of transition-metal complexes, we emphasize here that the nature of the coordinated ligands also has a strong influence over the spectral profiles.

In summary, the reaction of  $[1]^{2-}$  with 2 equiv of CN<sup>-</sup> yields the unusual, high-spin Co<sup>II</sup> complex  $[2]^{2-}$ , which provides structural insight toward the catalytically relevant intermediate  $[3]^{1-}$ . Compound  $[3]^{1-}$  is determined to be a monometallic Co<sup>II</sup>–superoxide complex supported by the redox non-innocent ligand L in its singly oxidized radical form. The local spin state of Co<sup>II</sup> is  $S = 3/2$ , but these electrons couple with unpaired electrons on L as well as the O<sub>2</sub><sup>-</sup> ligand to yield an overall  $S = 1/2$  state, as seen via EPR spectroscopy. The catalytic utility of  $[3]^{1-}$  is therefore attributable to its redox non-innocent L supporting ligand, allowing Co to remain high-spin upon activation of O<sub>2</sub> and avoiding the kinetic quagmire that is a low-spin Co<sup>III</sup> complex.

## ■ ASSOCIATED CONTENT

### Supporting Information

The Supporting Information is available free of charge on the ACS Publications website at DOI: 10.1021/jacs.5b12643.

Crystallographic data for  $[2]^{2-}$  (CIF)

Synthetic and spectroscopic methods, full MO diagrams,

Cartesian coordinates (PDF)

## ■ AUTHOR INFORMATION

### Corresponding Authors

\*kml236@cornell.edu

\*cora.macbeth@emory.edu

\*berry@chem.wisc.edu

### Present Address

<sup>†</sup>Department of Natural Sciences, Dalton State College

### Notes

The authors declare no competing financial interest.

## ■ ACKNOWLEDGMENTS

We thank NSF under the CCI for Selective C–H Functionalization for support (CHE-1205646). J.F.B. thanks the DOE (DE-FG02-10ER16204). K.M.L. thanks Cornell University for startup funding and NSF (CHE-1454455). A.R.C. thanks the NSF (DGE-0718123). R.C.W. thanks the NIH-NIGMS (T32GM008500). Computational (CHE-0840494) and EPR facilities (CHE-0741901) at UW-Madison are supported by NSF. We thank Dr. Elizabeth Blaesi for insightful discussions. This work is based on research conducted at the Cornell High Energy Synchrotron Source (CHESS), supported by NSF and NIH/NIGMS under NSF award DMR-1332208. EXAFS were measured at SSRL, which is supported by the U.S. Department of Energy, Office of Science, Office of Basic Energy Sciences under Contract No.

DE-AC02-76SF00515. The SSRL Structural Molecular Biology Program is supported by the Department of Energy's Office of Biological and Environmental Research, and by NIH/NIGMS (including P41GM103393).

## REFERENCES

- (1) (a) Werner, A.; Mylius, A. Z. *Anorg. Chem.* **1898**, *16*, 245. (b) Tsumaki, T. *Bull. Chem. Soc. Jpn.* **1938**, *13*, 252.
- (2) (a) Schaefer, W. P.; Marsh, R. E. *J. Am. Chem. Soc.* **1966**, *88*, 178. (b) Floriani, C.; Calderazzo, F. *J. Chem. Soc. A* **1969**, *6*, 946. (c) Rodley, G. A.; Robinson, W. T. *Nature* **1972**, *235*, 438. (d) Fritch, J. R.; Christoph, G. G.; Schaefer, W. P. *Inorg. Chem.* **1973**, *12*, 2170. (e) Collman, J. P.; Gagne, R. R.; Kouba, J.; Ljusberg-Wahren, H. *J. Am. Chem. Soc.* **1974**, *96*, 6800. (f) Gall, R. S.; Rogers, J. F.; Schaefer, W. P.; Christoph, G. G. *J. Am. Chem. Soc.* **1976**, *98*, 5135. (g) James, B. R. *The Porphyrins*; Dolphin, D., Ed.; Academic Press: New York, 1979; Vol. 5, pp 207–215. (h) Jones, R. D.; Summerville, D. A.; Basolo, F. *Chem. Rev.* **1979**, *79*, 139. (i) Bailey, C. L.; Drago, R. S. *Coord. Chem. Rev.* **1987**, *79*, 321. (j) Busch, D. H.; Alcock, N. W. *Chem. Rev.* **1994**, *94*, 585. (k) Hikichi, S.; Akita, M.; Moro-oka, Y. *Coord. Chem. Rev.* **2000**, *198*, 61. (l) Cho, J.-H.; Sarangi, R.; Kang, H.-Y.; Lee, J.-Y.; Kubo, M.; Ogura, T.; Solomon, E. I.; Nam, W.-W. *J. Am. Chem. Soc.* **2010**, *132*, 16977. (m) Tiné, M. R. *Coord. Chem. Rev.* **2012**, *256*, 316.
- (3) (a) Smith, T. D.; Pilbrow, J. R. *Coord. Chem. Rev.* **1981**, *39*, 295. (b) Mandal, A. K.; Iqbal, J. *Tetrahedron* **1997**, *53*, 7641. (c) Sharma, V. B.; Jain, S. L.; Sain, B. *Tetrahedron Lett.* **2003**, *44*, 383. (d) Schultz, M. J.; Sigman, M. S. *Tetrahedron* **2006**, *62*, 8227.
- (4) (a) Merckx, M.; Kopp, D. A.; Sazinsky, M. H.; Blazyk, J. L.; Müller, J.; Lippard, S. J. *Angew. Chem., Int. Ed.* **2001**, *40*, 2782. (b) Solomon, E. I.; Heppner, D. E.; Johnston, E. M.; Ginsbach, J. W.; Cirera, J.; Qayyum, M.; Kieber-Emmons, M. T.; Kjaergaard, C. H.; Hadt, R. G.; Tian, L. *Chem. Rev.* **2014**, *114*, 3659. (c) Wang, W.; Liang, A. D.; Lippard, S. J. *Acc. Chem. Res.* **2015**, *48*, 2632.
- (5) (a) Jazdzewski, B. A.; Tolman, W. B. *Coord. Chem. Rev.* **2000**, *200–202*, 633. (b) Meunier, B.; de Visser, S. I. P.; Shaik, S. *Chem. Rev.* **2004**, *104*, 3947. (c) Denisov, I. G.; Makris, T. M.; Sligar, S. G.; Schlichting, I. *Chem. Rev.* **2005**, *105*, 2253. (d) *Cytochrome P450: Structure, Mechanism, and Biochemistry*, 3rd ed.; Ortiz de Montellano, P. R., Ed.; Kluwer/Plenum: New York, 2005. (e) Rose, E.; Andrioletti, B.; Zrig, S.; Quelquejeu-Etheve, M. *Chem. Soc. Rev.* **2005**, *34*, 573. (f) Chirik, P. J.; Wieghardt, K. *Science* **2010**, *327*, 794.
- (6) Sharma, S. K.; May, P. S.; Jones, M. B.; Lense, S.; Hardcastle, K. I.; MacBeth, C. E. *Chem. Commun.* **2011**, *47*, 1827.
- (7) Patra, T.; Manna, S.; Maiti, D. *Angew. Chem., Int. Ed.* **2011**, *50*, 12140.
- (8) For examples of M–O<sub>2</sub> complexes that require hydrogen peroxide and excess base to perform stoichiometric deformylation, see: (a) Seo, M. S.; Kim, J. Y.; Annaraj, J.; Kim, Y.; Lee, Y.-M.; Kim, S.-J.; Kim, J.; Nam, W. *Angew. Chem., Int. Ed.* **2007**, *46*, 377. (b) Jo, Y.; Annaraj, J.; Seo, M. S.; Lee, Y.-M.; Kim, S. Y.; Cho, J.; Nam, W. *J. Inorg. Biochem.* **2008**, *102*, 2155. (c) Cho, J.; Sarangi, R.; Nam, W. *Acc. Chem. Res.* **2012**, *45*, 1321. (d) Cho, J.; Kang, H. Y.; Liu, L. V.; Sarangi, R.; Solomon, E. I.; Nam, W. *Chem. Sci.* **2013**, *4*, 1502. (e) Shokri, A.; Que, L. *J. Am. Chem. Soc.* **2015**, *137*, 7686.
- (9) For a Cu<sup>II</sup> end-on superoxide complex that is capable of stoichiometric deformylation but requires superoxide, not O<sub>2</sub>, see: (a) Donoghue, P. J.; Gupta, A. K.; Boyce, D. W.; Cramer, C. J.; Tolman, W. B. *J. Am. Chem. Soc.* **2010**, *132*, 15869. (b) Pirovano, P.; Magherusan, A. M.; McGlynn, C.; Ure, A.; Lynes, A.; McDonald, A. R. *Angew. Chem., Int. Ed.* **2014**, *53*, 5946. (c) Ure, A. D.; McDonald, A. R. *Synlett* **2015**, *26*, 2060.
- (10) Classification of reactive metal-oxygen species as electrophilic implies reactivity such as O-atom transfer, hydrogen atom abstraction, and electron transfer. Nucleophilic metal-oxygen species react with electron-deficient substrates such as 2-PPA to produce acetophenone.
- (11) The  $\tau_\delta$  value distinguishes between “pinched” tetrahedral and sawhorse geometries.  $\tau_\delta$  values close to 1.0 indicate tetrahedral geometry, while  $\tau_\delta$  values between 0.45–0.63 are best described as distorted sawhorse geometries, see: Reineke, M. H.; Sampson, M. D.; Rheingold, A. L.; Kubiak, C. P. *Inorg. Chem.* **2015**, *54*, 3211.
- (12) Nguyen, A. I.; Hadt, R. G.; Solomon, E. I.; Tilley, T. D. *Chem. Sci.* **2014**, *5*, 2874.
- (13) Nakamoto, K. *Infrared and Raman Spectra of Inorganic and Coordination Compounds. Part B: Applications in Coordination, Organometallic, and Bioinorganic Chemistry*; Wiley: New York, 1997.
- (14) (a) Nelson, K. J.; Giles, I. D.; Shum, W. W.; Arif, A. M.; Miller, J. S. *Angew. Chem., Int. Ed.* **2005**, *44*, 3129. (b) Scott, T. A.; Berlinguette, C. P.; Holm, R. H.; Zhou, H.-C. *Proc. Natl. Acad. Sci. U. S. A.* **2005**, *102*, 9741.
- (15) Pollock, C. J.; Delgado-Jaime, M. U.; Atanasov, M.; Neese, F.; DeBeer, S. *J. Am. Chem. Soc.* **2014**, *136*, 9453.
- (16) For calculations ruling out a possible Co<sup>III</sup> side-on peroxide assignment for [3]<sup>1-</sup>, see SI.
- (17) Hehre, W. J. R. L.; Schleyer, P. V. R.; Pople, J. A. *Ab Initio Molecular Orbital Theory*; Wiley: New York, 1986.
- (18) The ground state of [3]<sup>1-</sup> was also assessed with SORCI calculations (see SI).
- (19) (a) Tomson, N. C.; Williams, K. D.; Dai, X.; Sproules, S.; DeBeer, S.; Warren, T. H.; Wieghardt, K. *Chem. Sci.* **2015**, *6*, 2474. (b) Walroth, R. C.; Uebler, J. W. H.; Lancaster, K. M. *Chem. Commun.* **2015**, *51*, 9864.